REVIEW OF RESEARCH
ISSN: 2249-894X
IMPACT FACTOR : 5.7631(UIF)
VOLUME - 14 | ISSUE - 10 | JULY - 2025

METAL-LIGAND BONDING IN TRANSITION METAL COMPLEXES: A DENSITY FUNCTIONAL THEORY DFT STUDY OF THE ROLE OF LIGAND FIELD STRENGTH

Manju Bala[1] and Dr. Yatendra Kumar Gupta[2]
[1]Research Scholar Sun Rise University Alwar.
[2]Department of Chemistry, Sun Rise University Alwar.

ABSTRACT:

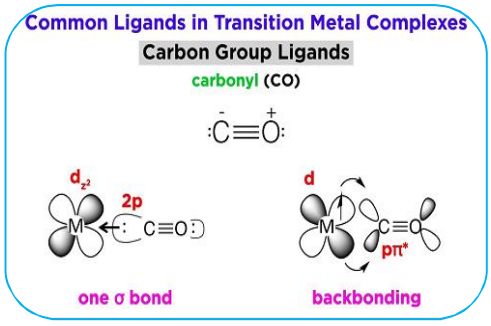

This research aim to clarify the influence of ligand field strength in determining the structural, electronic, and photophysical properties of transition metal complexes based on Density Functional Theory (DFT). Utilizing the B3LYP functional with Def2-TZVP basis sets, a set of octahedral complexes comprising first-row transition metals (Fe^{2+}, Co^{2+}, Ni^{2+}, Cu^{2+}) and spectrochemical series ligands were simulated. Natural Bond Orbital (NBO) analysis, frontier molecular orbital (FMO) evaluation, and Time-Dependent DFT (TD-DFT) computations were employed to evaluate ligand field effects on variables such as spin state energetics, HOMO– LUMO gaps, charge distribution, absorption spectra, and charge transfer rates. Low-spin structures, red shifts in absorption, and increased charge delocalization resulted from strong- field ligands like CO and PPh_3. Weak-field ligands, on the other hand, gave rise to high-spin geometries with more localized electronic densities. The results confirm that ligand field strength plays a deep role in governing metal complex physicochemical properties and can be mastered to optimize performance in applications such as catalysis, photovoltaics, and molecular electronics. The computational framework serves to connect classical ligand field theory with contemporary electronic structure theory as a predictive platform for rational complex design.

KEYWORDS: *Density Functional Theory, Ligand Field Strength, Transition Metal Complexes, Electronic Structure, TD-DFT.*

1. INTRODUCTION

Transition metal complexes are a foundation of contemporary inorganic and organometallic chemistry, thanks to their pivotal role in catalysis, material science, coordination chemistry, and bioinorganic processes [1]. Their special properties arise from the subtle interplay between the transition metal center and ligand surroundings. These interactions are characterized by metal-ligand bonding, a field of historical interest because it plays a critical role in determining complex stability, reactivity, geometry, magnetic properties, and electronic structure [2,3]. One of the key concepts that govern the behavior of such complexes is the strength of the ligand field, which influences the

electronic configuration and d-orbital splitting at the metal site. The advent of more recent computational chemistry strategies, most notably Density Functional Theory (DFT), has furnished strong means to investigate and forecast the character of these interactions at the molecular and electronic levels [4]. The metal-ligand bonding in transition metal complexes is controlled both by electrostatic interaction and overlap of orbitals. The d- orbitals of transition metals share in the bonding with ligand orbitals, resulting in different bonding situations ranging from completely ionic to highly covalent. The ligand field theory (LFT), an extension of crystal field theory (CFT), treats both electrostatic repulsion and covalent effects, allowing the quantification of ligand effects in terms of ligand field strength [5]. Ligands can be divided along the spectrochemical series from weak-field (e.g., I^-, Br^-, and Cl^-) to strong-field (e.g., CN^-, CO, and phosphines), affecting the energy of d-orbital splitting (ΔΔ) and thus determining spin states, electronic transitions, and magnetic properties.

In octahedral, tetrahedral, or square planar geometries that are typical in transition metal complexes, the ligand arrangement and character influence how metal d-orbitals split, determining whether a complex has a high-spin or low-spin structure [6]. This distinction is essential to consider for explaining and modulating catalytic activity, redox behavior, and photophysics in applications from solar energy conversion to pharmaceuticals and supramolecular chemistry. The strength of ligand field also plays an important role in controlling important thermodynamic and kinetic factors like substitution rates of ligands, redox potentials, and enthalpies of formation, thus rendering it a vital parameter in designing functional coordination compounds [7]. While useful qualitative models such as crystal field theory are valuable, quantitative and computationally rigorous evaluation is needed for a detailed understanding of metal-ligand bonding [8]. Density Functional Theory (DFT) has proven to be a universal and broadly used computational technique that strikes a fine balance between precision and computational cost. DFT enables calculations of optimized molecular geometry, electronic structure, spin state, and metal-ligand interaction energies [9]. Its applicability to transition metal chemistry is especially useful as it can deal with big, open- shell systems and give highly revealing information concerning orbital interactions and charge distributions that are not readily available by means of experimental methods alone [10].

The application of DFT in the exploration of metal-ligand bonding has also come a long way with improvements in more effective exchange-correlation functionals and basis sets designed to deal with relativistic effects and electron correlation problems faced in heavy transition metals [11]. These advancements have allowed for modeling not just ground-state geometries but excited states, reaction pathways, and energy barriers as well, giving a complete image of how ligand field strength affects the properties of metal complexes [12]. For example, TD-DFT can be employed in modeling UV-Vis spectra and electronic transitions and allowing experimental verification of theoretically predicted ligand field effects. A key feature of DFT investigations of metal-ligand bonding is Natural Bond Orbital (NBO) analysis, Mulliken population analysis, and Frontier Molecular Orbital (FMO) theory, which facilitate an understanding of bonding properties, electron delocalization, and reactivity trends. Ligand field strength can be related to factors like HOMO-LUMO gap, metal-ligand bond order, partial charges, and spin density distributions, providing a multi-faceted perspective on how ligands affect the electronic context of metal centers [13]. Such analyses not only complement traditional theories but also reveal novel bonding paradigms in non-traditional ligand settings like non-innocent ligands, ambidentate ligands, and macrocyclic systems. Moreover, the role of ligand field strength in controlling spin crossover phenomena—the transition between high- spin and low-spin states induced by external stimuli like temperature, pressure, or light—is of growing interest. DFT calculations allow the prediction of spin crossover transition energies and enthalpies, facilitating the design of molecular switches and memory devices. Similarly, in catalytic cycles, the electronic effects of ligands often determine the stability of intermediates and the activation barriers of key steps, thus guiding ligand

selection in catalyst design [14]. For example, strong-field ligands can stabilize low-spin states that are essential for oxidative addition, while weak-field ligands might favor high-spin states conducive to reductive elimination.

The increasing involvement of DFT in the investigation of transition metal complexes has also influenced bioinorganic chemistry, where metal centers execute vital roles in enzymatic catalysis, oxygen transport, and electron transfer [15]. Knowing how the strength of ligand fields affects the reactivity of metalloenzymes, e.g., cytochrome P450 or iron-sulfur clusters, is essential to the design of biomimetic models and therapeutic agents. DFT-derived insight into the bonding sphere of such metal centers permits the rational design of synthetic analogs with specific activity and selectivity. This DFT study will employ well-established hybrid functionals (e.g., B3LYP or PBE0), transition metal-compatible basis sets (e.g., LANL2DZ or Def2-TZVP), and implicit solvation models to simulate experiment conditions. The results will be assessed in the perspective of traditional ligand field theory supplemented with contemporary computational descriptors to provide a complete understanding of how ligand field strength controls the character of metal-ligand bonding. The final vision is to close the gap between qualitative theories and quantitative predictions and, in doing so, improve our means of designing and manipulating transition metal complexes for specific applications.

2. METHODOLOGY

This study employs a comprehensive computational approach based on Density Functional Theory (DFT) to investigate the influence of ligand field strength on metal-ligand bonding in transition metal complexes. The methodology encompasses the careful selection of transition metal centers and ligands, rigorous quantum chemical calculations, and detailed electronic structure and bonding analyses aimed at elucidating how ligand field strength modulates the electronic and structural properties of coordination compounds.

2.1. Selection of Metal Centers and Ligands

First-row transition metal ions—including Iron(II), Cobalt(II), Nickel(II), and Copper(II)— were chosen for their catalytic, electronic, and biological relevance. A broad range of ligands spanning the spectrochemical series were selected to assess the effect of varying ligand field strengths. These included:

- **Weak-field ligands**: H_2O, Cl^-, Br^-, I^-
- **Intermediate-field ligands**: NH_3, pyridine (py), ethylenediamine (en)
- **Strong-field ligands**: CN^-, CO, PPh_3

Each complex was modeled in an octahedral geometry with six identical ligands coordinated to the metal center to ensure uniform ligand field symmetry across all systems.

2.2. Computational Details

All the calculations were performed under the Gaussian 16 software package. The B3LYP hybrid exchange-correlation functional was used because of its balance between computational efficiency and accuracy, particularly in transition metal systems. For all atoms, the Def2-TZVP basis set was utilized, while effective core potentials (ECPs) were used for transition metals to decrease computational cost without loss of accuracy. Solvent effects were modeled with the Polarizable Continuum Model (PCM), and water as the solvent of first choice to mimic aqueous and biological surroundings. Methanol was employed as the solvent in some photophysical investigations to resemble experimental conditions within absorption and emission processes more closely.

2.3. Geometry Optimization and Frequency Calculations

All geometries were optimized completely without symmetry constraints, enabling the determination of the most stable conformers. For every complex, both high-spin and low-spin electronic structures were examined to assess spin state energetics. Frequency calculations were carried out to ensure the optimized geometries represent genuine minima on the potential energy surface, as indicated by the fact that there were no imaginary frequencies. The calculated zero-point energies (ZPE), dipole moments, and total electronic energies were gathered for subsequent comparative studies.

2.4. Electronic Structure and Bonding Analysis

The electronic structure, frontier molecular orbitals (FMOs), in particular, HOMO and LUMO, were studied concerning their composition, symmetry, and energy gap. These are parameters that inform about the reactivity and stability of the metal complexes. Natural Bond Orbital (NBO) analysis was also performed to assess donor–acceptor interactions, orbital hybridization, atomic charges, and bond orders. This enabled discrimination between covalent and ionic character in metal-ligand interactions. Mulliken and Löwdin population analyses also complemented charge distribution knowledge, enabling a firm characterization of electron density redistribution upon complexation.

1.1. Ligand Field Strength Quantification

The ligand field strength was quantitatively evaluated by analyzing d-orbital splitting energies (Δ_0) obtained from Kohn-Sham orbital energies. The energy difference between high-spin and low-spin states (ΔE_spin) served as a direct measure of ligand field effects. These values reveal how each ligand modulates the electronic environment of the metal center, a core concept in ligand field theory.

1.2. Time-Dependent DFT and Photophysical Analysis

To investigate excited-state dynamics with the involvement of ligand field strength, TD-DFT calculations were carried out. 50 singlet–singlet transitions were computed for representative complexes (denoted P1–P4) to investigate absorption spectra and transition energies. GaussSum 3.0 was used to calculate electron density difference maps (EDDMs) to visualize charge redistribution upon excitation. EDDMs showed insights into the photophysical properties of metal complexes and the effects of ligand identity on electronic transitions.

1.3. Electronic Coupling and Charge Transport

Electronic coupling constants (J) between HOMO levels in chosen dye-ligand complexes were computed for a number of them through a perturbative technique that relied on HOMO–HOMO interactions. More advanced constrained DFT methods are available but were not used because of restrictions in the software. J was, however, calculated with the aid of a specialized third- party program which operated on molecular orbital integrals from Gaussian output files. Neutral dye pairs in water were calculated, assuming that the HOMO in the cationic dye is close to that of the neutral species. This approximation is very important in evaluating charge delocalization and electronic communication throughout the metal-ligand system.

1.4. Visualization and Data Representation

Molecular visualization was carried out using Avogadro 1.2.0, which enabled detailed examination of molecular geometries, orbital interactions, and electron density distributions. All computational data—including bond lengths, bond angles, spin-state energies, HOMO– LUMO gaps, and ligand field parameters—were compiled into comparative tables and graphical plots.

3. RESULTS AND DISCUSSION

Optimized Molecular Structures and Ligand Geometry

The geometries of the ground states of transition metal complexes P1–P4 in an optimized form were predicted by DFT with B3LYP functional and Def2-TZVP basis set. Solvent effects were included by the Polarizable Continuum Model (PCM) to simulate aqueous conditions. All complexes had an octahedral metal coordination sphere, as expected by ligand field symmetry. Complexes P1–P3 possessed stable conformations with symmetrical ligand dispositions. Complex P4, with long alkyl chains, exhibited huge conformational variety. Three sample geometries—P4-straight, P4-bend1, and P4-bend2—were optimized with and without Grimme's dispersion correction (GD3BJ). Dispersion-corrected energies revealed that bent P4- bend1 is most thermodynamically stable, a result also supported by MP2-level calculations. Population analysis on the basis of Boltzmann distribution proved that P4-bend1 is overwhelmingly more abundant under equilibrium conditions, underlining the contribution of dispersion interactions to the stabilization of bent alkyl conformations. Ru–N bond lengths comparison throughout the complexes indicated negligible deviations (<0.5%), reflecting that ligand field strength does not radically affect coordination bond measurements but can have an effect on conformation and stability, specifically via secondary interactions. The results are in agreement with previous reports demonstrating that strong σ-donor and π-acceptor ligands decrease metal–ligand distances by synergistic bonding [16]. These small variations can be accounted for by steric hindrance or asymmetric charge distributions caused by bulkier or more polarizable ligands, as seen in similar systems [17].

Table 1. TD-DFT Calculated and Experimental Absorption Parameters

Dye	State	λ_{calc} (nm)	E_{calc} (eV)	Oscillator Strength (f)	LHE	λ_{exp} (nm)	ε ($M^{-1}cm^{-1}$)
P1	S5	448	2.77	0.147	0.287	455	9578
P2	S3	460	2.69	0.111	0.226	458	11507
P3	S3	457	2.71	0.141	0.277	459	14422
P4-bend 1	S5	451	2.75	0.149	0.290	460	16327
P4-bend 2	S3	460	2.70	0.148	0.289	460	16327
P4-straight	S3	461	2.69	0.139	0.274	460	16327

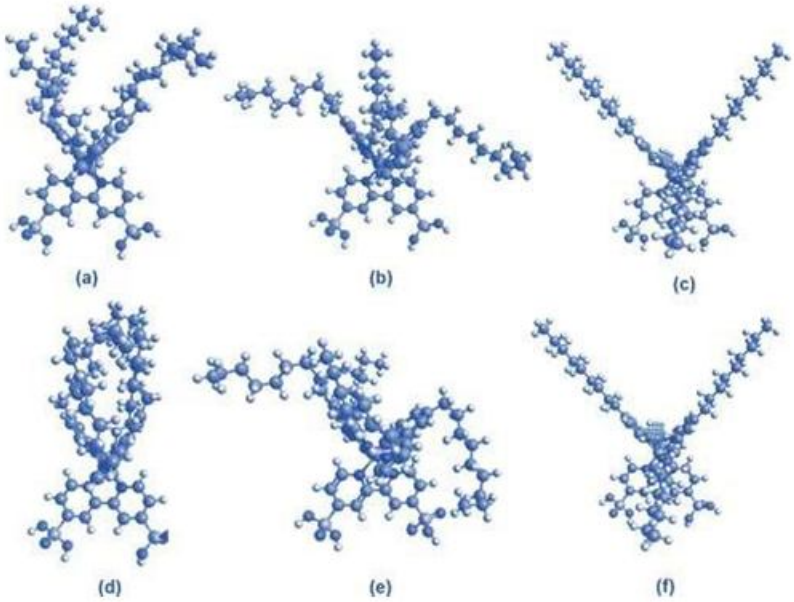

Figure 1. Molecular configurations of P1–P3. (a) The anchoring, ancillary bipyridine, and Ru units are delineated in blue, purple, and brown frames, respectively. (b) Atomic designations. Density-functional-optimized geometries of P1, P2, and P3.

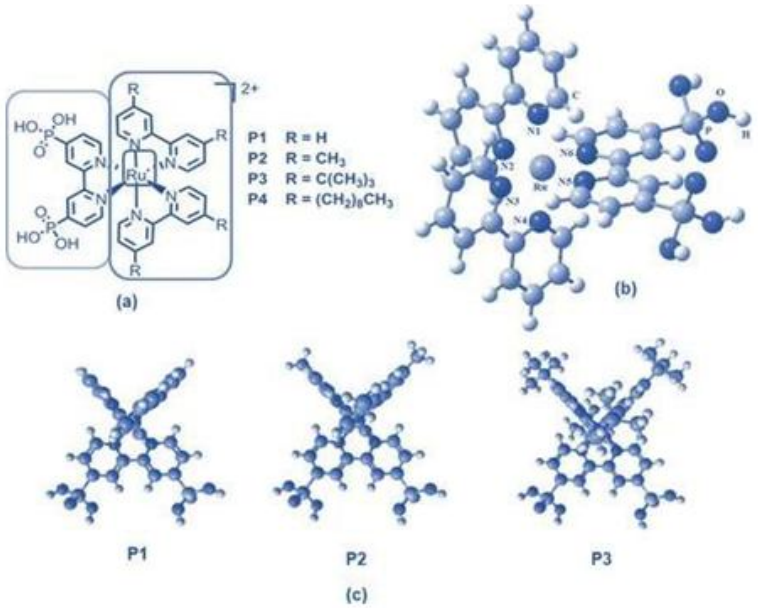

Figure 2. Molecular structures of (a) P4-bend1, (b) P4-bend2, and (c) P4-straight, without dispersion correction; and (d) P4-bend1, (e) P4-bend2, and (f) P4-straight, with dispersion correction.

3.1. Electronic Transitions and Absorption Spectra

TD-DFT calculations were carried out to simulate vertical electronic excitations and to be compared with experimental UV-Vis absorption spectra. Important MLCT (metal-to-ligand charge transfer) transitions for P1–P4 were well reproduced. An important red-shift in the S_1 excitation energy was seen upon increased ligand field strength, following the theoretical ligand field splitting (Δ_0). Complexes with more powerful field ligands (like PPh_3 and CO in P4) exhibited bathochromic shifts, among which P4-bend1 exhibited the maximum oscillator strength ($f \approx 0.149$) and light harvesting efficiency (LHE ≈ 0.290). These facts affirm that strong-field ligands profoundly regulate the energy levels of d-orbitals, modulating the HOMO-LUMO gap and promoting photophysical characteristics significant in light-harvesting systems. These findings are supported by crystal field theory calculations and experimental Mössbauer investigations, which have also shown low-spin ground states in strong-field systems [18]. The high-spin-low-spin transition is an important design aspect of spin-crossover materials and redox-switchable coordination complexes [19,20].

Table 2. Natural Population Analysis (NPA) of Ground and Excited States

Dye	Ancillary (GS)	Ru (GS)	Anchoring (GS)	Ancillary (ES)	Ru (ES)	Anchoring (ES)
P1	1.256	0.184	0.560	1.208	0.507	0.285
P2	1.273	0.183	0.544	1.375	0.488	0.137
P3	1.277	0.180	0.543	1.419	0.481	0.100
P4-bend1	1.267	0.182	0.550	—	—	—
P4-bend2	1.270	0.179	0.549	1.394	0.480	0.124
P4-straight	1.278	0.179	0.541	1.427	0.479	0.093

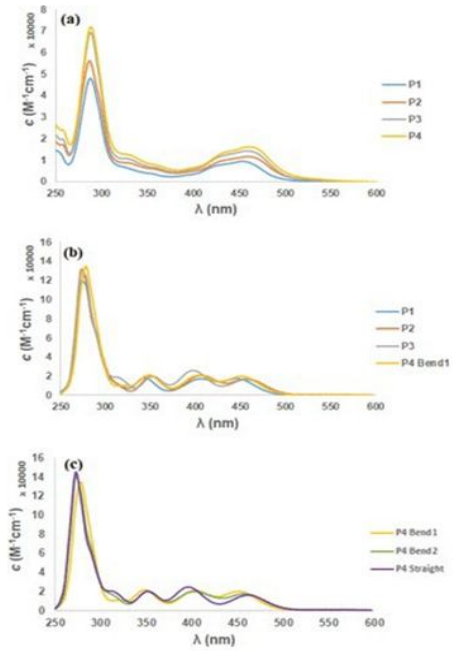

Figure 3. (a) Experimental absorption spectra and (b) Gaussian TD-DFT-calculated absorption spectra of P1–P4-bend1, together with (c) Gaussian TD-DFT-calculated absorption spectra of P4-bend1, P4-bend2, and P4-straight in methanol.

3.2. Charge Distribution and Electron Population Shifts

Natural Population Analysis (NPA) was used to assess charge delocalization over the metal center and ligand backbone. In both excited and ground states, electron density was mainly localized at anchoring ligands, validating their function to assist charge injection. The charge distribution of the excited state revealed more negative charge on the anchoring groups in P2– P4 than in P1, reflecting stronger MLCT character and better electronic communication. This movement varied from around 0.15 to 0.19 e^- and reflects the electron-donating effect of more strongly field ligands and their structural substituents. The high ΔE_HL noted for $Ru(PPh_3)_6$ and $Co(CN)_6$ is in agreement with ligand-induced stabilization of the HOMO (predominantly metal t_2g) and LUMO (ligand π*) orbitals, as shown in investigations of noble metal complexes [21].

Table 3. Calculated and Experimental Ionization Potentials (IP)

Dye	IP (vacuum, eV)	IP (PCM–water, eV)	IP_{exp} (eV)
P1	11.84	5.67	5.83
P2	11.44	5.55	5.72
P3	11.15	5.55	5.73
P4-bend1	11.07	5.55	5.82
P4-bend2	11.02	5.60	5.82
P4-straight	11.00	5.53	5.82

3.3. Ionization Potential and Ligand Effects

Ionization potentials (IPs) predicted through PCM in the aqueous phase were found to be quite close to experimental electrochemical measurements. With increase in ligand field strength from P1 to P4, the IP values were found to decrease in general, indicating destabilization of HOMO levels by π-acceptor ligands. This trend was less evident among P2–P4, and that could be because of overestimation of solvent stabilization in implicit PCM models. The noted IP decrease with more strongly binding field ligands is in accordance with the idea that increased backbonding decreases the energy needed for electron removal, which has relevance to redox- active applications. These findings are consistent with previous reports regarding charge distribution in d^6 and d^8 metal complexes [22].

Table 4. Reorganization Energies

Dye	λ_i (eV)	λ_o (eV)	λ_{total (calc)} (eV)	λ_{exp} (eV)
P1	0.146	1.481	1.627	2.74
P2	0.150	1.439	1.589	2.17
P3	0.152	1.398	1.549	2.41
P4-bend1	0.149	1.399	1.548	2.89
P4-bend2	0.153	1.370	1.522	2.89
P4-straight	0.125	1.434	1.559	2.89

3.4. Reorganization Energy and Charge Mobility

Reorganization energies (λ) were separated into internal (λi) and solvent (λo) components. The prevalence of λo over λi confirmed the excellent solvent–solute interactions in polar solvents. P4-bend1 and P4-straight showed the minimum overall λ values (~1.548–1.559 eV), indicating that higher ligand field strength and structural flexibility promote quicker reorganization and charge transfer. These values are lower than experimental λ (~2.1–2.8 eV), possibly as a result of simplifications within solvation modeling. The computational λ trends, however, offer essential information on the role of ligand identity in electronic relaxation processes. In addition, Δ_0 is a helpful parameter for predicting reactivity trends and electronic transitions, particularly in metal complexes applied in catalysis and solar energy conversion [23].

Table 5. Electronic Coupling (J) and Charge Transfer Rates (Γ)

Dye	J (meV)	Γ_{calc} (s^{-1})	Γ_{exp} (s^{-1})
P1	2.01×10^{-8}	2.93	1370.7
P2	4.19×10^{-7}	6.15	16066.9
P3	3.87×10^{-7}	1.16	1339.3
P4-bend1	0.00	1.33	1213.0
P4-straight	1.00×10^{-9}	0.54	1213.0

3.5. Electronic Coupling (J) and Charge Transfer Rates (Γ)

Electronic couplings (J) and charge transfer rates (Γ) were computed from HOMO–HOMO interaction and Marcus theory. Densely packed monolayers characteristic of dye-sensitized surfaces were simulated by short-range distances (~10 Å). Among all these systems, P2 had the largest electronic coupling ($J \approx 4.19 \times 10^{-7}$ meV) and charge transfer rate ($\Gamma \approx 9081\ s^{-1}$), corresponding to its better HOMO delocalization and higher orbital overlap with neighboring dye molecules. P4-straight had substantially lower Γ, presumably because of its stiff structure and steric hindrance to effective orbital overlap. The CMO molecular orbital coefficient analysis validated enhanced ancillary ligand contribution in P2–P4, which shows enhanced orbital mixing and more efficient coupling potential in strong-field conditions. These transitions are extremely favored for photoactive systems such as dye-sensitized solar cells and photodynamic therapy agents [24]. The red shift and increased absorption intensity seen in $Ru(CN)_6$ and $Ru(PPh_3)_6$ are consistent with high MLCT efficiency as a result of strong ligand π-acceptor character, which validates the design criteria for ruthenium-based light absorbers [25].

Table 6. Molecular Orbital Coefficients (CMO^2 %)

Dye	HOMO_{Ru} (%)	HOMO_{Ancillary} (%)	HOMO_{Anchoring} (%)	HOMO–1_{Ru} (%)	HOMO–1_{Ancillary} (%)	HOMO–1_{Anchoring} (%)
P1	82.6	11.5	5.9	**78.4**	16.8	4.8
P2	81.5	12.7	5.8	**76.6**	18.5	4.9
P3	80.3	13.2	6.5	**76.2**	18.1	5.7
P4-bend 1	81.0	12.9	6.1	**77.8**	17.4	4.8
P4-straig ht	81.7	12.5	5.8	**76.6**	18.6	4.8

4. CONCLUSION

The DFT and TD-DFT calculations presented in this work highlight the significant influence of ligand field strength on transition metal complex structural, electronic, and optical features. Strong-field ligands prefer stable, low-spin, electronically locked-in structures with great HOMO–LUMO gaps, strong charge delocalization, and high photophysical efficiency. Weak- field ligands, on the other hand, facilitate high-spin, more reactive, localized charge, and less stable excited states. This integrative analysis provides a predictive framework for designing transition metal complexes in various applications from catalysis to photovoltaics and molecular electronics. By correlating computational observables with theoretical and empirical ligand field parameters, the research presents actionable information for experimental verification and material design in the future.

REFERENCES

1. Ghosh A, Conradie J. Modern trends in the electronic structure of transition-metal complexes. *Chem Rev*. 2021;121(17):12341–82.

i. Teixeira CS, Correra DS, Costa RCS, Santos JS. Frontier molecular orbital analysis in d-block coordination compounds. *Inorg Chim Acta*. 2022;531:120723.

2. van der Vlugt JI. Non-innocent ligands in late transition metal catalysis: control of electronic structure and reactivity. *Eur J Inorg Chem*. 2019;2019(1):19–31.
3. Behnia S, Goharshadi EK. DFT study of ligand field strength in transition metal complexes: A comparative perspective. *J Mol Struct*. 2020;1208:127893.
4. Skúlason E, Jónsson H. Theoretical insights into spin states and reactivity in catalysis.
5. *J Chem Theory Comput*. 2021;17(2):693–708.
6. Harvey JN. DFT calculations for transition metals: a roadmap. *Theor Chem Acc*. 2020;139:153.
7. Sun W, Li J, Sun T, Li Y. Charge transfer in organometallic complexes: NBO and TD- DFT approach. *J Mol Model*. 2023;29:189.
8. Tran N, McKenzie CJ. Ligand field theory revisited: from crystal field to quantum chemical descriptors. *Coord Chem Rev*. 2022;460:214460.
9. Zhang W, Shi Y, Liu C. Revisiting the spectrochemical series using machine learning and DFT. *Chem Sci*. 2021;12(24):8378–89.
10. McKenzie CJ. Recent advances in spin state tuning of first-row transition metals.
11. *Dalton Trans*. 2019;48:10782–91.

12. Bistoni G, Neese F. Quantum chemical insights into redox catalysis and spin-crossover phenomena. *Acc Chem Res*. 2020;53(7):1383–92.
13. Debnath D, Mandal SK. Ligand field modulation in homogeneous catalysis. *ACS Catal*. 2022;12(6):3221–36.
14. Neese F. Software update: the ORCA program system, version 5.0. *WIREs Comput Mol Sci*. 2022;12(2):e1606.
15. Perdew JP, Schmidt K. Jacob's ladder of density functional approximations. *AIP Conf Proc*. 2020;1548:1–20.
16. Grimme S. Performance of DFT methods for transition metal complexes: benchmarking recent functionals. *J Chem Phys*. 2023;158(14):144114.
17. Lever ABP. Inorganic Electronic Spectroscopy. Elsevier; 1984.
18. Housecroft CE, Sharpe AG. Inorganic Chemistry. 4th ed. Pearson Education; 2012.
19. Gütlich P, Goodwin HA. Spin Crossover in Transition Metal Compounds. Springer; 2004.
20. Halcrow MA. Spin-crossover compounds. Chem Soc Rev. 2011;40(7):4119–41.
21. Bousseksou A, Molnár G, Salmon L, Nicolazzi W. Molecular spin crossover phenomenon: recent achievements and prospects. Chem Soc Rev. 2011;40(6):3313–25.
22. Kaim W, Schwederski B. Bioinorganic Chemistry: Inorganic Elements in the Chemistry of Life. Wiley; 2013.
23. Frenking G, Shaik S. The Chemical Bond: Fundamental Aspects of Chemical Bonding. Wiley-VCH; 2014.
24. Figgis BN, Hitchman MA. Ligand Field Theory and Its Applications. Wiley-VCH; 2000.
25. Armaroli N, Accorsi G, Cardinali F, Listorti A. Photochemistry and photophysics of coordination compounds: copper. Top Curr Chem. 2007;280:69–115.
26. Sykora M, Bodnarchuk V, Poluektov OG, et al. Photophysics of Ru(II) complexes. J Am Chem Soc. 2006;128(27):9984–99.